Suppressors of cGAS-STING are downregulated during fin-limb regeneration and aging in aquatic vertebrates

Sabateeshan Mathavarajah[1], Andrew W. Thompson[2,3,4], Matthew R. Stoyek[5], T. Alexander Quinn[5,6], Stéphane Roy[7], Ingo Braasch[3,4], Graham Dellaire*[1,8]

[1]Department of Pathology, Faculty of Medicine, Dalhousie University, Halifax, NS, Canada
[2]Department of Biological Sciences, Western Michigan University, Kalamazoo, MI, USA.
[3]Department of Integrative Biology, Michigan State University, East Lansing, MI, USA.
[4]Ecology, Evolution, and Behavior Program, Michigan State University, East Lansing, MI, USA.
[5]Department of Physiology and Biophysics, Dalhousie University, Halifax, Canada
[6]School of Biomedical Engineering, Dalhousie University, Halifax, Canada
[7]Department of Stomatology, Faculty of Dentistry, Université de Montréal, Montréal, QC, Canada.
[8]Department of Biochemistry and Molecular Biology, Dalhousie University, Halifax, NS, Canada

*Corresponding authors:

Dr. Graham Dellaire
Department of Pathology and Department of Biochemistry and Molecular Biology
Halifax, Nova Scotia, Canada
dellaire@dal.ca

Keywords: cGAS-STING, Limb regeneration, Fin regeneration, PML, Plex9.1, TREX1

Abbreviations: cGAS, cyclic guanosine monophosphate–adenosine monophosphate synthase; STING, stimulator of interferon genes; PML, Promyelocytic Leukemia; Plex9.1, PML-like exon 9.1, TREX1, Three prime repair exonuclease 1; cGAMP, Cyclic guanosine monophosphate–adenosine monophosphate

Abstract

During the early stages of limb and fin regeneration in aquatic vertebrates (i.e. fishes and amphibians) blastema undergo transcriptional rewiring of innate immune signalling pathways to promote immune cell recruitment. In mammals, a fundamental component of innate immune signalling in mammals is the cytosolic DNA sensing pathway, cGAS-STING. However, to what extent the cGAS-STING pathway influences regeneration in aquatic anamniotes is unknown. In jawed vertebrates, negative regulation of cGAS-STING activity is accomplished by suppressors of cytosolic DNA such as Trex1, Pml and PML-like exon 9 (Plex9) exonucleases. Here, we examine the expression of these suppressors of cGAS-STING, as well as inflammatory genes and cGAS activity during caudal fin and limb regeneration using the spotted gar (*Lepisosteus oculatus*) and axolotl (*Ambystoma mexicanum*) model species, and during age-related senescence in zebrafish (*Danio rerio*). In the regenerative blastema of wounded gar and axolotl, we observe increased inflammatory gene expression, including interferon genes and interleukins 6 and 8. We also observed a decrease in axolotl *Trex1* and gar *pml* expression during the early phases of wound healing which correlates with a dramatic increase in cGAS activity. In contrast, the *plex9.1* gene does not change in expression during wound healing in gar. However, we observed decreased expression of *plex9.1* in the senescing cardiac tissue of aged zebrafish, where 2′3′-cGAMP levels are elevated. Finally, we demonstrate a similar pattern of *Trex1, pml and plex9.1* gene regulation across species in response to exogenous 2′3′-cGAMP. Thus, during the early stages of limb-fin regeneration, Pml, Trex1 and Plex9.1 exonucleases are downregulated, presumably to allow an evolutionarily old cGAS-STING activity to promote inflammation and the recruitment of immune cells.

Introduction

Tissue regeneration occurs in many different animal species, with the capacity for regeneration varying significantly among even highly related animals (Alibardi, 2017; Brockes & Gates, 2014; Dwaraka & Voss, 2021; Goss & Holt, 1992; McLaughlin, Rathbone, Liversage, & McLaughlin, 1983; Nogueira et al., 2016; Simon & Tanaka, 2013; Tomlinson, Tomlinson, & Tassava, 1985). Not only do these different vertebrate species share an ability to regenerate but there is an overlap in the molecular pathways involved in regeneration between the early blastema of ray-finned fish and lobe-finned vertebrates (Darnet et al., 2019). For example, the transcriptional changes are remarkably similar during the early stages of tetrapod limb and actinopterygian fin regeneration between bichir (*Polypterus senegalus)* and axolotl (Darnet et al., 2019) in pathways that control inflammatory responses and innate immune signalling (e.g., interferon a [IFNa]-like signalling). These pathways are critical for the recruitment of macrophages and other immune cells to the wound (Brockes & Gates, 2014; Darnet et al., 2019; Godwin, Pinto, & Rosenthal, 2013; Nogueira et al., 2016).

In addition to inflammation, numerous cellular pathways are involved in facilitating the wound healing response such as the proliferation of progenitor cells, the maintenance of their genome integrity, cell differentiation with positional memory, extracellular matrix remodelling and the prevention of apoptosis (McCusker et al., 2015). Key signalling proteins and their respective pathways such as fibroblast growth factors, bone morphogenetic proteins, and Wnt, all contribute to the process (McCusker et al., 2015). Intriguingly, DNA damage response associated genes are also activated in response to regeneration in these model systems (Darnet et al., 2019). The DNA damage response is critical for early blastema proliferation during vertebrate regeneration, presumably as a contributor to downstream immune signalling during wound healing (Garcia-Lepe, Cruz-Ramirez, & Bermudez-Cruz, 2021; Garcia-Lepe, Torres-Dimas, Espinal-Centeno, Cruz-Ramirez, & Bermudez-Cruz, 2022; Sousounis et al., 2020).

Innate immunity and the DNA damage response are united through the highly conserved cyclic GMP-AMP synthase - stimulator of interferon response cGAMP interactor 1 (cGAS-STING) pathway (Hopfner & Hornung, 2020; T. Li & Chen, 2018). The cGAS-STING axis is activated to promote interferon (IFN) stimulated gene expression in response to stress in the form of viral infection, DNA damage, mitochondrial dysfunction, and long interspersed nuclear element 1 (LINE-1) retroelement expression (Hopfner & Hornung, 2020; T. Li & Chen, 2018; Maekawa et al., 2019; Ni, Ma, & Damania, 2018). Linking all of these activators of cGAS-STING is the sensing of cytosolic DNA; for example, DNA damage response proteins either directly (e.g. MUS81, MRE11) or indirectly sense cytosolic DNA *via* other DNA sensors like IFI16 (e.g. PARP1), which together contribute to activate cGAS-STING induce the expression of type I IFN genes (reviewed in (Hopfner & Hornung, 2020) and (Lin, Tang, & Zheng, 2022)).

In mammals, the cGAS-STING pathway is also involved in the early stages of wound healing and regeneration of the peripheral nervous system, liver and intestinal wall in mammals, where it contributes to the inflammation and the recruitment of macrophages to the site of injury (Leibowitz et al., 2021; Morozzi et al., 2021; X. Wang et al., 2023). During mammalian regeneration, *CGAS* expression is upregulated to promote STING-dependent innate immune signalling (Morozzi et al., 2021). During mammalian aging, cGAS-STING is also associated

with the activation of the senescence-associated secretory phenotype (SASP), and expression of inflammatory cytokines such as interleukin 6 and 8 (*IL6, IL8*) which can promote aging (Hopfner & Hornung, 2020; Hui Yang, Hanze Wang, Junyao Ren, Qi Chen, & Zhijian J Chen, 2017).

Several additional observations from aquatic models suggest that cGAS-STING has an evolutionarily conserved role: During axolotl regeneration, progenitor limb blastema cells secrete IL-8 (Tsai, Baselga-Garriga, & Melton, 2019) and STING-dependent IL-6 signalling (C. Wang et al., 2023) is one of the most enriched overlapping pathways between fin and limb regeneration (Darnet et al., 2019). Finally, similar changes in inflammatory gene expression have also been observed in zebrafish, where immune cells accumulate in elderly animals in response to STING, with numerous chemokines being upregulated (Reuter et al., 2022). This phenomenon has been termed "inflammaging", and the age-related activation of endogenous retroelements such as LINE-1 in senescent cells can promote further aging by inducing additional IFN and inflammatory cytokine production through the cGAS-STING pathway (Andrade et al., 2022; Schmitz, Maurmann, Guma, Bauer, & Barbe-Tuana, 2023). Taken together, the cGAS-STING axis plays a critical role in tissue homeostasis, facilitating both tissue regeneration and senescence in both mammals and aquatic anamniotes.

Although DNA sensors are important for activating cGAS-STING, the molecular "brakes" on this pathway are just as important for tissue homeostasis. A key brake on cGAS-STING is mammalian TREX1, an exonuclease that degrades cytoplasmic DNA and suppresses LINE-1 to prevent cGAS activation (Ablasser et al., 2014; Mathavarajah, Salsman, & Dellaire, 2019; Thomas et al., 2017). Recently, we showed that in aquatic vertebrates, the promyelocytic leukemia (Pml) protein and newly discovered DEDDh exonucleases known as PML-like exon 9 (Plex9) proteins can suppress the cGAS-STING pathway through their exonuclease function and through exonuclease-independent suppression of LINE-1, akin to mammalian TREX1 (Mathavarajah et al., 2023). Despite the known role of cGAS-STING in wound healing and tissue regeneration discussed above, it remains unclear the extent to which the exonuclease suppressors of this pathway play a deeply conserved role in tissue regeneration in other vertebrate species, or if the pathway is an evolutionary innovation of the mammalian lineage.

Here, we survey the expression of inflammatory genes in three different anamniote species, including fin and limb regeneration in the non-teleost fish spotted gar (*Lepisosteus oculatus*) and the amphibian axolotl (*Ambystoma mexicanum*), and during zebrafish (*Danio rerio*) cardiac aging. Taken together, our results indicate that Pml, Plex9.1, and Trex1 share strikingly similar gene regulation in these aquatic vertebrate species during regeneration and aging, where they are downregulated to promote cGAS-STING activity and downstream pro-inflammatory signalling. This suggests an evolutionary old function of cGAS-STING program that evolved in fish ancestor of living jawed vertebrates, if not earlier.

Methods

Cell Lines and 2'3'-cGAMP treatment

Previously derived cell lines from the longnose gar, *Lepisosteus osseus* (GARL, liver derived fibroblasts (F. Liu, Bols, Pham, Secombes, & Zou, 2019)), axolotl (AL-1 limb dermal

fibroblast derived cell line (Denis, Sader, Ferretti, & Roy, 2015)) and zebrafish (ZKS, zebrafish kidney stromal cells (Stachura et al., 2009)) were used. Gar-L cells were maintained in Leibovitz L15 (L-15) medium supplemented with 10% newborn bovine calf serum (NCBS, New Zealand origin, ThermoFisher), and 1% Pen/Strep (100 U/ml penicillin and 100 µg/mL streptomycin) in CO2-independent and dark conditions. AL-1 cells were grown in a mixed media (62.5% MEM (Gibco) and 25% water) with 10% fetal bovine serum (ThermoFisher) supplemented with 100 U penicillin-streptomycin, glutamine, and insulin within a humidified incubator at 25°C with 2% CO2. ZKS cells were maintained in culture media consisting of 10% fetal bovine serum (FBS; ThermoFisher), 55% L-15, 32.5% Dulbecco modified Eagle medium (DMEM) (Gibco) and 12.5% Ham F-12 (Gibco). ZKS media was supplemented with 150 mg/L sodium bicarbonate, 2% penicillin/streptomycin (10 U/mL stock), 1.5% N-2-hydroxyethylpiperazine-N′-2-ethanesulfonic acid (HEPES), 1% l-glutamine and 0.1 mg/mL gentamycin. ZKS cells were grown at 32°C and 5% CO2. 2′3′-cGAMP (InvivoGen) was transfected into cells using Lipofectamine 2000 (Invitrogen) or JetPRIME (PolyPlus) at 100ng or 2 µg. Untreated cells received the Lipofectamine 2000 or JetPRIME lacking 2′3′-cGAMP. For conditioned media experiments, cells were transfected, and then media was collected 48 hours later. The conditioned media was added to fresh media at a ratio of 1:1 and the naïve cells were incubated for 24 hours, after which, RNA was collected. All cell lines were passaged at a 1:2 split when cells reached 80-90% confluency.

Regeneration experiments

Spotted Gar (n-12, 19-25cm standard length) were anesthetized in 160mg/L MS-222 (Sigma) and caudal fins were amputated via a vertical cut using the ventral apex as a landmark to begin the cut. This amputated, posterior part of the caudal fin from 0dpa was put in RNA later and stored at -80C. Gar with amputated fins were monitored until a time of secondary sampling at 7dpa (n=4), 16dpa (n=4), and 32dpa (n=4) upon which time the regenerating caudal fin was sampled under anesthesia by via another vertical cut anterior to the initial 0dpa cut site. This resulted in a thin strip of fin tissue (up to ~1cm in width) that contained original caudal fin tissue as well as all regenerated tissue up to that time point. Day 0 samples were collected for all animals and then matched to the animals for each timepoint when regenerating tissue was later collected. Thus, we refer to day 0 as Amputated Fin (AF) for each individual animal and the re-sampled regenerative blastema as Regenerative Blastema (RB) throughout the manuscript. All 7dpa, 16dpa, and 32dpa tissues was put in RNA later and stored at -80C. All gars were euthanized at the end of the experiment in 300mg/L MS-222.

The axolotl limbs were amputated at the level of the zeugopod (forearm, through the radius and ulna bones) under anesthesia using buffered MS222 0.1X dissolved in 40% Holtfreter's solution. Blastema from the regenerating limb were then isolated at different stages of the regenerating bud (early - ~6 days post amputation; medium – 8-9 days post amputation; late - 10-12 days post amputation)(Stocum, 1979).

RNA extractions from isolated tissue

Dissected tissues were lysed and homogenized using Trizol reagent (Thermo) according to the manufacturer's directions and frozen at -80°C for further analysis. Blastema RNA from gar and axolotl were isolated from single tissue samples. Hearts were pooled from 3 animals for

zebrafish samples. Zebrafish included young adult (6-10 months post fertilization) and aged (20-24 months post fertilization) cohorts. The samples were then processed for RNA using the Ambion PureLink RNA Mini Kit (Thermo) according to the manufacturer's protocol and an on-column DNase I digestion. Quality and quantity of RNA was measured using a Nanodrop 2000 spectrophotometer (Thermo). Absorbance measurements A260/A280 and A260/A230 with ratios ~2.0 were accepted for downstream analysis by RT-qPCR.

RT-qPCR

cDNA was generated from 1 µg of RNA (for axolotl) or 500 ng of RNA (for zebrafish and spotted gar) using the BioRad 5X iScript RT supermix kit (BioRad Laboratories Canada; Mississauga, ON, CA) for RT-qPCR, after which samples were diluted 1:1 with nuclease-free water. Control samples lacking reverse transcriptase were included to confirm no genomic DNA contamination. Quantitative PCR (qPCR) was performed on cDNA samples using the 2X SsoAdvanced Universal SYBR Green Supermix (BioRad). The reactions were performed using BioRad CFX Connect and all experiments were done in triplicate. Primers were designed using NCBI Primer Blast (**https://www.ncbi.nlm.nih.gov/tools/primer-blast/**) and are included in Supplementary Table 1. Gene expression data were normalized to at least two reference genes from each species (spotted gar –*actb* and *gapdh*; axolol – *gapdh* and *rpl4*; zebrafish - *rplp0* and *actb1*) and analyzed using the BioRad CFX Maestro Software. Data were collected and analyzed as per the MIQE guidelines (Bustin et al., 2009).

2'3'- cGAMP quantification

Gar blastema and axolotl blastema were weighed, washed 3x with PBS and then lysed using M-PER (Thermo Scientific). Individual zebrafish hearts were washed 3x with PBS, homogenized using a grinder and then lysed using M-PER. Lysates were incubated on ice for 30 minutes with gentle agitation every 10 minutes, before being spun down with 16,000 x g at 4° C for 10 min. Samples were quantified using a 2′3′-cGAMP ELISA kit (Cayman Chemical) according to the manufacturer's instructions.

Immunohistochemistry

For immunofluorescence assessment of the presence and distribution of γ-H2AX in the zebrafish heart, ventricles were isolated from zebrafish expressing eGFP under the myocyte-specific *myl7* promoter (*tg(myl7:eGFP)*) for visualisation of the cardiac musculature. As previously described (Stoyek, Rog-Zielinska, & Quinn, 2018), the hearts were fixed overnight in 4% paraformaldehyde (Electron Microscopy Sciences) with 1% DMSO (Sigma-Aldrich) in phosphate-buffered saline (Sigma-Aldrich). The hearts were then rinsed three times for 15 min each in PBS and transferred to a solution containing 0.1% Triton X-100 (PBS-T; T9284, Sigma-Aldrich) in PBS with mouse monoclonal anti-H2a.x (1:100; JBW301; Millipore) and incubated for 3 days with agitation at 4ºC. Tissues were rinsed three times for 15 min each in PBS-T and transferred to PBS-T containing the appropriate secondary antibody (1:300, AlexaFluor555; A-21429, Fisher Scientific) for 2 days with agitation at 4ºC. Final rinsing was done in PBS and specimens were placed in Scale CUBIC-R1 clearing solution (Susaki et al., 2014) overnight at room temperature with gentle agitation. Ventricles were sectioned roughly in half with midline

cut on the axial plane and hearts were then mounted on glass slides in CUBIC-R1 for confocal microscopy. Processed specimens were examined as whole-mounts using an LSM 710 confocal microscope using Zeiss Zen software (Carl Zeiss, Toronto, Canada).

Animal ethics

Spotted gar work was approved by the Institutional Animal Care and Use Committee at Michigan State University (protocol no. PROTO201900309). All the experiments done with axolotls were approved by the Université de Montréal institutional animal care committee in accordance with the Canadian Council on Animal Care. All experimental procedures with zebrafish were approved by the Dalhousie University Committee for Laboratory Animals (protocol number 20-074) and followed the guidelines of the Canadian Council on Animal Care.

Statistical analyses

For statistical analyses between groups of 3 or more (for gar, axolotl and cell line experiments), significance was determined using a One-way ANOVA, with Tukey's post-hoc analysis used for comparison. For zebrafish aging experiments where comparison was made between 2 cohorts, significance was determined using a Student's t-test (two-tailed). All statistical analyses were completed using GraphPad Prism 9.

Results

Immune signalling is upregulated in the early stages of gar caudal fin regeneration

We examined regenerative blastema isolated from spotted gar at various stages of caudal fin regeneration and assessed whether innate immune signalling associated genes differed in expression (Figure 1A). We found changes to Ifn genes such as *ifnb* and *ifnc1*, which were upregulated ~98-fold and ~96-fold respectively at the earliest stage of 7 days post-amputation (7 dpa) (Figure 1B). In addition, orthologs of inflammatory interleukins Il6 and Il8, were also found to be significantly upregulated 7 dpa in the regenerative blastema. By 16 dpa, *ifnb, ifnc1*, *il6* and *il8* returned to baseline levels.

Since cGAS-STING is a conserved regulator of type I IFNs and interleukins such as IL6 and IL8 in mammals (Chernyavskaya et al., 2017; Ge et al., 2015; Glück et al., 2017), we next measured cGAS activity in our gar model by measuring the levels of 2′3′-cGAMP, the product of cGAS. Consistent with cGAS-STING activation, we found that the 7 dpa blastema had significantly elevated amounts of 2′3′-cGAMP (Figure 1C). However, the expression of cGAS and STING orthologs in the gar fin regenerative blastema did not significantly change. We next surveyed two recently identified suppressor proteins of cGAS activity in gar, Plex9.1 and Pml (Mathavarajah et al., 2023). While we observed no changes to *plex9.1* expression, there was a ~8-fold reduction in *pml* gene expression at 7 dpa.

Cross-species conservation of cGAS-STING activation in early stages of regeneration

We next examined inflammatory gene expression, cGAS-STING activity, and the expression of cGAS suppressors during axolotl limb regeneration. First, we measured the gene expression of axolotl *il6* and *il8* in tissue isolated from regenerating axolotl at the early stages of regeneration (timepoints of 0h, 6h, 24h, 48h, 96h) and at three major stages of limb regeneration (i.e. the early, medium and late bud stage) (Figure 2A). Intriguingly, *il8* was significantly upregulated within the first 48 hours of regeneration and remained elevated throughout the medium and late bud stage (Figure 2B). In contrast, *il6* was upregulated within 96 hours (Figure 2B) and remained elevated only through the early bud stage.

We then assessed cGAS activity and found elevated levels of 2′3′-cGAMP only during the early bud stage of limb regeneration (Figure 2C). Similar to the gar regenerative blastema, we did not observe significant changes in the expression of axolotl *cgas* or *sting* during the 4 days of wound healing or at the different limb bud stages (Figure 2D). Since the axolotl genome does not encode *plex9.1* or *pml* paralogs (Mathavarajah et al., 2023), we next examined the expression of axolotl Trex1, which suppresses axolotl cGAS-STING as in mammals (Figure 2E) (2). We observed a significant and immediate ~48-fold decrease in *Trex1* gene expression in the blastema within 6 hours of limb removal, with *Trex1* expression only restored at the late bud stage (Figure 2D). Collectively, these data indicate that during limb-fin regeneration, Trex1 and Pml, appear to be downregulated to promote type I IFN signalling during regeneration in axolotl and gar, respectively.

Plex9 enzymes have elevated expression in the cardiac tissue of aged fish

The Plex9.1 enzyme is also capable of suppressing cGAS-STING (Mathavarajah et al., 2023); however, we did not observe significant changes in Plex9.1 expression during gar regeneration. Therefore, we sought to determine if Plex9.1 may be differentially regulated to influence cGAS-STING signalling in another biological process, such as aging. During aging, the cGAS-STING pathway promotes SASP and inflammatory cytokine expression that underlies cellular senescence (Hui Yang et al., 2017). However, since the spotted gar is collected from wild spawns, we used the laboratory spawned and maintained zebrafish model for comparing young versus elderly fish. Another experimental advantage of the zebrafish and other teleost fishes is a lack of orthologs for either Pml and Trex1 (Mathavarajah et al., 2023), making it an ideal model to observe *plex9.1* gene expression and its impact on cGAS-STING activity without overlapping contributions of Pml and Trex1 to cGAS suppression.

Zebrafish Plex9.1 expression is highest in the adult heart (data not shown) and for that reason, we used hearts from young and elderly zebrafish as our model for studying cGAS-STING in senescence. When we examined the hearts of aged zebrafish for STING-dependent immune signalling genes, we found elevated levels of *ifnphi1*, *il8* and *isg15* (Figure 3A). Similarly, markers of senescence such as *p21* and *p53* were also upregulated in the hearts of elderly fish (Figure 3B). In addition, γH2AX, a cellular senescence marker, is upregulated in the

elderly fish cardiomyocytes (Figure 3C). When we examined cGAS activity in hearts from young versus aged zebrafish, we found significantly increased levels of 2′3′-cGAMP in the hearts from aged animals (Figure 3D). However, we did not observe changes in either *cgasa* or *sting1* expression relative to age (Figure 3E), and we could not detect any *cgasb* expression in cardiac tissue. In contrast, we did observe a ~68-fold drop in *plex9.1* expression between the young and aged zebrafish hearts (Figure 3E).

Pml, plex9.1 and Trex1 are downregulated in response to 2′3′-cGAMP

Since spotted gar *pml* and axolotl *Trex1* expression is reduced during the early stages of fin and limb regeneration, and zebrafish *plex9.1* expression is reduced in the cardiac tissue of aged zebrafish, we hypothesized that 2′3′-cGAMP may play a feedback role in controlling the expression of these suppressors of cGAS-STING. To address this hypothesis, we employed cell culture models derived from gar, axolotl and zebrafish (GARL, AL-1 and ZKS cells, respectively) to decipher which stimuli alter *pml*, *Trex1* and *plex9.1* expression. We transfected cells with 2′3′-cGAMP at low (100 ng) and high (2 µg) concentrations to activate the cGAS-STING pathway and examined gene expression of the exonucleases. We found that in gar, axolotl and zebrafish cells, *pml*, *Trex1* and *plex9.1* gene expression (respectively) decreased in response to low 2′3′-cGAMP levels (Figure 3F). However, at higher concentration of 2′3′-cGAMP, the expression of all three enzymes significant increased. This increase in exonuclease expression at higher 2′3′-cGAMP concentrations, however, did not correspond to further changes in the expression of interferon or senescence-associated genes from each species (Supplementary Figure 1). Thus, 2′3′-cGAMP levels and therefore resulting the activity of cGAS, directly impacts the gene expression of *pml, Trex1* and *plex9.1*.

We also further examined if the cGAMP response we observed was cell intrinsic or had a paracrine signalling component in the three species. For these experiments, we focused on *interleukin 8* (*Il8*) expression as it was significantly upregulated in response to aging and regeneration across the three species, and in response to low dose 2′3′-cGAMP treatment (Supplementary Figure 2). Consistent with a paracrine component to the cGAMP response, conditioned media from transfected cells when applied to naïve untreated cells, induced a significant increase in *Il8* expression in the gar, zebrafish and axolotl cells (Supplementary Figure 2). There was no significant difference between incubation with conditioned media and transfection with 2′3′-cGAMP for zebrafish and axolotl (Supplementary Figure 1). However, while we observed a ~15-fold increase in *il8* expression in response to cGAMP treatment in gar cells, conditioned media elicited an attenuated but significant increase of only ~5 fold (Supplementary Figure 2). Although the reason for the reduced *il8* induction in gar cells treated with conditioned media is unclear, we do note that gar cells are grown at room temperature which we speculate may affect secretion of paracrine factors.

Discussion

The spotted gar was recently shown to be capable of regenerating its caudal fin after amputation to the endoskeleton (Darnet et al., 2019). In axolotl, a similar regenerative blastema is associated with activation of innate immune signalling (Darnet et al., 2019), however, it is unclear whether activation of innate immune signalling in regenerative blastema is conserved

across species. We found that the early stage of regenerative blastema in the spotted gar and axolotl share similarities in the transcriptional changes that promote STING-dependent immune signalling during regeneration. Specifically, Il-6 and Il-8, two key cytokines expressed in response to STING activation are upregulated in both gar and axolotl regenerative blastema (Figure 1 and 2). Il-8 was recently shown to be essential for axolotl limb regeneration (Tsai et al., 2019), and IL-6 is a well-established factor involved in mammalian liver regeneration, which has been shown to also be involved fin regeneration in axolotl and bichir (Streetz, Luedde, Manns, & Trautwein, 2000). Therefore, there is conserved reprogramming of regenerative blastema towards a highly active innate immune signalling state in the early stages of spotted gar fin regeneration, similar to what has been observed in other species capable of regeneration.

The similar upregulation of both in early gar fin regeneration seen in the current study suggests that STING activity is increased by cells at the site of injury is a conserved program across bony vertebrates, which corresponds to an increase in 2′3′-cGAMP as we observed in gar blastema (Figure 2). However, while not examined in the current study, it is possible that the downregulation of exonucleases could impact other DNA-based sensors in the cytoplasm. This could include AIM2 that promotes inflammatory signalling via the inflammasome after sensing (Motwani et al., 2019). In addition, sensing of RNA could also influence this process as the RNA sensor RIG-I has been shown to promote type I IFN signalling during intestinal regeneration in mice (Fischer et al., 2015). While we establish cGAS as a contributing factor to limb-fin regeneration, more work is required to understand how these other sensors could also be involved in vertebrate tissue regeneration.

IFN genes likely arose in the earliest jawed vertebrates, as these genes are present in extant cartilaginous and bony fish (Redmond, Zou, Secombes, Macqueen, & Dooley, 2019). Paralogous genes representing all three IFN subgroups (I-III) can be found in the spotted gar genome (Braasch et al., 2016) In a gar cell line, IFNc1 but not IFNb paralogs are upregulated in response to viral mimicry using poly (I:C) treatment that activates IFN gene expression *via* the retinoic acid inducible gene I (RIG-I) pattern recognition receptor and the mitochondrial antiviral signalling protein (MAVS) (F. Liu et al., 2019). However, here, both IFNc1 and IFNb are expressed in the regenerative blastema, which is regulated by cGAS activation (Figure 1). Thus, in gar it appears that IFNc1 responds to both viral mimicry and fin damage, whereas IFNb expression is specific to wound healing and cGAS activation. In the future, it will be of interest to determine if these differences in IFN gene regulation can be exploited to further explore the evolutionary conservation of specialized innate immune responses to different cell stresses (viral infection, DNA damage, wound healing) and their corresponding pattern recognition receptors in early jawed vertebrates.

In fishes, the cGAS-STING pathway has been shown to play an important role in their antiviral and antibacterial immune responses (de Oliveira Mann et al., 2019; Z. F. Liu et al., 2020; Sellaththurai et al., 2023). Our results extend these observations to the conservation of cGAS-STING function in tissue regeneration and aging. Moreover, we also provide the first data regarding the regulation of key suppressors of cGAS (Pml, Trex1 and Plex9.1) in jawed vertebrates during wound healing and aging. Specifically, during ray-finned fish and amphibian fin and limb regeneration, we demonstrate that the expression of *pml*, *Trex1* and *plex9.1* is tied to the activity of cGAS, providing a potential feedback mechanism to potentiate or dampen

downstream IFN and senescence gene regulation (Figure 3). Importantly, our study demonstrates that in diverse bony vertebrates the cellular response to tissue damage or aging appears to rely on the initial downregulation of suppressor exonucleases, to promote cGAS-STING signalling.

Another important element of these conserved responses to tissue damage and aging, is the contribution of specific cell types to inflammatory signalling during injury and regeneration. Although there is little published work on *plex9.1* and *pml* regarding tissue level expression in zebrafish and gar, we did find that *Trex1* is specifically expressed in the epithelial cells of different axolotl tissues (Ye et al., 2022). Thus, it appears that epithelial cells are likely important players in initiating inflammatory signalling through cGAS-STING within damaged tissues, but generalization of these data to other species requires further study.

We also observe that key cytokines involved in inflammaging (i.e. IL6 and IL8) are upregulated in our aquatic vertebrate models during both tissue regeneration (Figure 1 and 2) and aging (Figure 3). The secretion of cGAMP-stimulated factors contributes to induction of interferon and senescencerelated genes in the cell lines derived from the different animals (Supplementary Figure 2). This is consistent with the fact that a significant number of cells at the site of injury senesce (H. Li et al., 2021). These cells are then cleared by macrophages after their recruitment (H. Li et al., 2021). In addition, recent work on axolotl limb regeneration has revealed that senescent cells create a pro-proliferative niche for progenitor cell expansion and blastema outgrowth (Yu et al., 2022). Thus, cGAS-STING activation and cGAS suppressor downregulation during regeneration promotes cell senescence while simultaneously creating an environment primed for immune cell recruitment and tissue remodelling.

Previous work identified *plex9.1* among the downregulated genes during cardiomyocyte regeneration akin to *pml* during gar caudal fin regeneration (Wu et al., 2015). We observe that ray-finned fish *plex9.1*, which functions akin to tetrapod Trex1 (Mathavarajah et al., 2023) is also downregulated in the hearts of aged zebrafish, which correlates to elevated cGAS activity (Figure 3). This is consistent with Plex9.1 playing a potentially important role in maintaining cardiac function in teleost fish during aging, as previous work found that mice lacking Trex1 exhibit severe inflammatory myocarditis, cardiomyopathy and eventually circulatory failure (Morita et al., 2004; Stetson, Ko, Heidmann, & Medzhitov, 2008). Thus, the reduced expression of cGAS suppressor enzymes likely contributes to normal biological aging and senescence across different bony vertebrate species (De Cecco et al., 2019; H. Yang, H. Wang, J. Ren, Q. Chen, & Z. J. Chen, 2017). The de-repression of retroelements also occurs during aging and can activate cGAS (De Cecco et al., 2019). For example, LINE-1 retroelements were recently shown to promote the senescence associated secretory phenotype through the activation of cGAS-STING (De Cecco et al., 2019). Previously, we have demonstrated that Pml, Trex1 and Plex9.1 collectively suppress LINE retroelements as an exonuclease-independent function to limit cGAS activation (Mathavarajah et al., 2023). Considering that cardiac tissue from older zebrafish had higher levels of 2′3′-cGAMP, coupled with a decrease in cGAS-suppressor *plex9.1* expression, the activation of cGAS-STING in senescing cells seems to be a conserved pathologic process in vertebrates.

In the future, we anticipate that the comparative biomedical investigation of aquatic vertebrate model systems such as the gar, zebrafish and axolotl will provide a useful experimental paradigm for studying the co-evolution of endogenous retroelements and the genes

that suppress their pathological consequences during development, regenerative wound healing and aging.

Funding

This work was funded by Discovery Grants from the Natural Sciences and Engineering Research Council of Canada [NSERC, RGPIN 2020-04034 to G.D; and RGPIN-2022-03150 to T.A.Q.]; G.D. is a senior scientist of the Beatrice Hunter Cancer Research Institute (BHCRI); S.M. is a trainee in the Cancer Research Training Program of the BHCRI, with funds provided by GIVETOLIVE and The Linnea Veinotte Memorial Graduate Studentship. S.M. is also supported by a Nova Scotia Graduate Scholarship, a Killam Doctoral Award and a Dalhousie University's Presidents Award. Gar work is supported by NIH [R01OD011116]; NSF EDGE program award [2029216 to I.B.].

Acknowledgements

We would like to thank Dr. David Stachura (California State University, Chico) and Dr. Neils C. Bols (University of Waterloo) for the gift of zebrafish and gar cell lines (respectively). We also thank Brett Racicot (Michigan State University) for spotted gar husbandry and facility management.

References

1. Ablasser, A., Hemmerling, I., Schmid-Burgk, J. L., Behrendt, R., Roers, A., & Hornung, V. (2014). TREX1 deficiency triggers cell-autonomous immunity in a cGAS-dependent manner. *The Journal of Immunology, 192*(12), 5993-5997.
2. Alibardi, L. (2017). Hyaluronic acid in the tail and limb of amphibians and lizards recreates permissive embryonic conditions for regeneration due to its hygroscopic and immunosuppressive properties. *Journal of Experimental Zoology Part B: Molecular and Developmental Evolution, 328*(8), 760-771. doi:https://doi.org/10.1002/jez.b.22771
3. Andrade, B., Jara-Gutierrez, C., Paz-Araos, M., Vazquez, M. C., Diaz, P., & Murgas, P. (2022). The Relationship between Reactive Oxygen Species and the cGAS/STING Signaling Pathway in the Inflammaging Process. *Int J Mol Sci, 23*(23). doi:10.3390/ijms232315182
4. Braasch, I., Gehrke, A. R., Smith, J. J., Kawasaki, K., Manousaki, T., Pasquier, J., ... & Postlethwait, J. H. (2016). The spotted gar genome illuminates vertebrate evolution and facilitates human-teleost comparisons. *Nature genetics*, *48*(4), 427-437.
5. Brockes, J. P., & Gates, P. B. (2014). Mechanisms underlying vertebrate limb regeneration: lessons from the salamander. *Biochem Soc Trans, 42*(3), 625-630. doi:10.1042/BST20140002
6. Bustin, S. A., Benes, V., Garson, J. A., Hellemans, J., Huggett, J., Kubista, M., . . . Wittwer, C. T. (2009). The MIQE guidelines: minimum information for publication of quantitative real-time PCR experiments. *Clin Chem, 55*(4), 611-622. doi:10.1373/clinchem.2008.112797
7. Chernyavskaya, Y., Mudbhary, R., Zhang, C., Tokarz, D., Jacob, V., Gopinath, S., . . . Sadler, K. C. (2017). Loss of DNA methylation in zebrafish embryos activates retrotransposons to trigger antiviral signaling. *Development, 144*(16), 2925-2939. doi:10.1242/dev.147629
8. Darnet, S., Dragalzew, A. C., Amaral, D. B., Sousa, J. F., Thompson, A. W., Cass, A. N., . . . Schneider, I. (2019). Deep evolutionary origin of limb and fin regeneration. *Proc Natl Acad Sci U S A, 116*(30), 15106-15115. doi:10.1073/pnas.1900475116
9. De Cecco, M., Ito, T., Petrashen, A. P., Elias, A. E., Skvir, N. J., Criscione, S. W., . . . Sedivy, J. M. (2019). L1 drives IFN in senescent cells and promotes age-associated inflammation. *Nature, 566*(7742), 73-78. doi:10.1038/s41586-018-0784-9
10. de Oliveira Mann, C. C., Orzalli, M. H., King, D. S., Kagan, J. C., Lee, A. S. Y., & Kranzusch, P. J. (2019). Modular Architecture of the STING C-Terminal Tail Allows Interferon and NF-kappaB Signaling Adaptation. *Cell Rep, 27*(4), 1165-1175 e1165. doi:10.1016/j.celrep.2019.03.098
11. Fischer, J. C., Bscheider, M., Eisenkolb, G., Wintges, A., Lindemans, C. A., Heidegger, S., ... & Poeck, H. (2015). RIG-I-induced type I IFNs promote regeneration of the intestinal stem cell compartment during acute tissue damage. *Blood*, *126*(23), 3072.
12. Denis, J. F., Sader, F., Ferretti, P., & Roy, S. (2015). Culture and transfection of axolotl cells. *Methods Mol Biol, 1290*, 187-196. doi:10.1007/978-1-4939-2495-0_15
13. Dwaraka, V. B., & Voss, S. R. (2021). Towards comparative analyses of salamander limb regeneration. *J Exp Zool B Mol Dev Evol, 336*(2), 129-144. doi:10.1002/jez.b.22902
14. Garcia-Lepe, U. O., Cruz-Ramirez, A., & Bermudez-Cruz, R. M. (2021). DNA repair during regeneration in Ambystoma mexicanum. *Dev Dyn, 250*(6), 788-799. doi:10.1002/dvdy.276
15. Garcia-Lepe, U. O., Torres-Dimas, E., Espinal-Centeno, A., Cruz-Ramirez, A., & Bermudez-Cruz, R. M. (2022). Evidence of requirement for homologous-mediated DNA repair during Ambystoma mexicanum limb regeneration. *Dev Dyn, 251*(6), 1035-1053. doi:10.1002/dvdy.455
16. Ge, R., Zhou, Y., Peng, R., Wang, R., Li, M., Zhang, Y., . . . Wang, C. (2015). Conservation of the STING-Mediated Cytosolic DNA Sensing Pathway in Zebrafish. *J Virol, 89*(15), 7696-7706. doi:10.1128/JVI.01049-15

17. Glück, S., Guey, B., Gulen, M. F., Wolter, K., Kang, T. W., Schmacke, N. A., . . . Ablasser, A. (2017). Innate immune sensing of cytosolic chromatin fragments through cGAS promotes senescence. *Nat Cell Biol, 19*(9), 1061-1070. doi:10.1038/ncb3586
18. Godwin, J. W., Pinto, A. R., & Rosenthal, N. A. (2013). Macrophages are required for adult salamander limb regeneration. *Proc Natl Acad Sci U S A, 110*(23), 9415-9420. doi:10.1073/pnas.1300290110
19. Goss, R. J., & Holt, R. (1992). Epimorphic vs. tissue regeneration in Xenopus forelimbs. *Journal of Experimental Zoology, 261*(4), 451-457. doi:https://doi.org/10.1002/jez.1402610412
20. Hopfner, K.-P., & Hornung, V. (2020). Molecular mechanisms and cellular functions of cGAS–STING signalling. *Nature reviews Molecular cell biology, 21*(9), 501-521.
21. Leibowitz, B. J., Zhao, G., Wei, L., Ruan, H., Epperly, M., Chen, L., . . . Yu, J. (2021). Interferon b drives intestinal regeneration after radiation. *Sci Adv, 7*(41), eabi5253. doi:10.1126/sciadv.abi5253
22. Li, H., Wei, X., Zhou, L., Zhang, W., Wang, C., Guo, Y., . . . Xu, X. (2021). Dynamic cell transition and immune response landscapes of axolotl limb regeneration revealed by single-cell analysis. *Protein Cell, 12*(1), 57-66. doi:10.1007/s13238-020-00763-1
23. Li, T., & Chen, Z. J. (2018). The cGAS–cGAMP–STING pathway connects DNA damage to inflammation, senescence, and cancer. *Journal of Experimental Medicine, 215*(5), 1287-1299.
24. Lin, F., Tang, Y. D., & Zheng, C. (2022). The crosstalk between DNA damage response components and DNA-sensing innate immune signaling pathways. *Int Rev Immunol, 41*(2), 231-239. doi:10.1080/08830185.2021.1898605
25. Liu, F., Bols, N. C., Pham, P. H., Secombes, C. J., & Zou, J. (2019). Evolution of IFN subgroups in bony fish - 1:Group I-III IFN exist in early ray-finned fish, with group II IFN subgroups present in the Holostean spotted gar, Lepisosteus oculatus. *Fish & Shellfish Immunology, 95*, 163-170. doi:https://doi.org/10.1016/j.fsi.2019.10.032
26. Liu, Z. F., Ji, J. F., Jiang, X. F., Shao, T., Fan, D. D., Jiang, X. H., . . . Shao, J. Z. (2020). Characterization of cGAS homologs in innate and adaptive mucosal immunities in zebrafish gives evolutionary insights into cGAS-STING pathway. *FASEB J, 34*(6), 7786-7809. doi:10.1096/fj.201902833R
27. Maekawa, H., Inoue, T., Ouchi, H., Jao, T.-M., Inoue, R., Nishi, H., . . . Tanaka, Y. (2019). Mitochondrial damage causes inflammation via cGAS-STING signaling in acute kidney injury. *Cell reports, 29*(5), 1261-1273. e1266.
28. Mathavarajah, S., Salsman, J., & Dellaire, G. (2019). An emerging role for calcium signalling in innate and autoimmunity via the cGAS-STING axis. *Cytokine Growth Factor Rev, 50*, 43-51. doi:10.1016/j.cytogfr.2019.04.003
29. Mathavarajah, S., Vergunst, K. L., Habib, E. B., Williams, S. K., He, R., Maliougina, M., . . . Dellaire, G. (2023). PML and PML-like exonucleases restrict retrotransposons in jawed vertebrates. *Nucleic Acids Res*. doi:10.1093/nar/gkad152
30. McCusker, C., Bryant, S. V., & Gardiner, D. M. (2015). The axolotl limb blastema: cellular and molecular mechanisms driving blastema formation and limb regeneration in tetrapods. *Regeneration*, 2(2), 54-71.
31. McLaughlin, H. M. G., Rathbone, M. P., Liversage, R. A., & McLaughlin, D. S. (1983). Levels of cyclic GMP and cyclic AMP in regenerating forelimbs of adult newts following denervation. *Journal of Experimental Zoology, 225*(2), 175-185. doi:https://doi.org/10.1002/jez.1402250202
32. Morita, M., Stamp, G., Robins, P., Dulic, A., Rosewell, I., Hrivnak, G., . . . Barnes, D. E. (2004). Gene-targeted mice lacking the Trex1 (DNase III) 3'-->5' DNA exonuclease develop inflammatory myocarditis. *Mol Cell Biol, 24*(15), 6719-6727. doi:10.1128/MCB.24.15.6719-6727.2004

33. Morozzi, G., Rothen, J., Toussaint, G., De Lange, K., Westritschnig, K., Doelemeyer, A., . . . Fornaro, M. (2021). STING regulates peripheral nerve regeneration and colony stimulating factor 1 receptor (CSF1R) processing in microglia. *iScience, 24*(12), 103434. doi:10.1016/j.isci.2021.103434
34. Motwani, M., Pesiridis, S., & Fitzgerald, K. A. (2019). DNA sensing by the cGAS–STING pathway in health and disease. *Nature Reviews Genetics*, *20*(11), 657-674.
35. Ni, G., Ma, Z., & Damania, B. (2018). cGAS and STING: At the intersection of DNA and RNA virus-sensing networks. *PLoS pathogens, 14*(8), e1007148.
36. Nogueira, A. F., Costa, C. M., Lorena, J., Moreira, R. N., Frota-Lima, G. N., Furtado, C., . . . Schneider, I. (2016). Tetrapod limb and sarcopterygian fin regeneration share a core genetic programme. *Nat Commun, 7*, 13364. doi:10.1038/ncomms13364
37. Redmond, A. K., Zou, J., Secombes, C. J., Macqueen, D. J., & Dooley, H. (2019). Discovery of All Three Types in Cartilaginous Fishes Enables Phylogenetic Resolution of the Origins and Evolution of Interferons. *Front Immunol, 10*, 1558. doi:10.3389/fimmu.2019.01558
38. Reuter, H., Perner, B., Wahl, F., Rohde, L., Koch, P., Groth, M., . . . Englert, C. (2022). Aging Activates the Immune System and Alters the Regenerative Capacity in the Zebrafish Heart. *Cells, 11*(3). doi:10.3390/cells11030345
39. Schmitz, C. R. R., Maurmann, R. M., Guma, F., Bauer, M. E., & Barbe-Tuana, F. M. (2023). cGAS-STING pathway as a potential trigger of immunosenescence and inflammaging. *Front Immunol, 14*, 1132653. doi:10.3389/fimmu.2023.1132653
40. Sellaththurai, S., Jung, S., Kim, M. J., Nadarajapillai, K., Ganeshalingam, S., Jeong, J. B., & Lee, J. (2023). CRISPR/Cas9-Induced Knockout of Sting Increases Susceptibility of Zebrafish to Bacterial Infection. *Biomolecules, 13*(2). doi:10.3390/biom13020324
41. Simon, A., & Tanaka, E. M. (2013). Limb regeneration. *Wiley Interdiscip Rev Dev Biol, 2*(2), 291-300. doi:10.1002/wdev.73
42. Sousounis, K., Bryant, D. M., Martinez Fernandez, J., Eddy, S. S., Tsai, S. L., Gundberg, G. C., . . . Whited, J. L. (2020). Eya2 promotes cell cycle progression by regulating DNA damage response during vertebrate limb regeneration. *Elife, 9*. doi:10.7554/eLife.51217
43. Stachura, D. L., Reyes, J. R., Bartunek, P., Paw, B. H., Zon, L. I., & Traver, D. (2009). Zebrafish kidney stromal cell lines support multilineage hematopoiesis. *Blood, 114*(2), 279-289. doi:10.1182/blood-2009-02-203638
44. Stetson, D. B., Ko, J. S., Heidmann, T., & Medzhitov, R. (2008). Trex1 prevents cell-intrinsic initiation of autoimmunity. *Cell, 134*(4), 587-598. doi:10.1016/j.cell.2008.06.032
45. Stocum, D. L. (1979). Stages of forelimb regeneration in Ambystoma maculatum. *Journal of Experimental Zoology, 209*(3), 395-416. doi:https://doi.org/10.1002/jez.1402090306
46. Stoyek, M. R., Rog-Zielinska, E. A., & Quinn, T. A. (2018). Age-associated changes in electrical function of the zebrafish heart. *Progress in Biophysics and Molecular Biology, 138*, 91-104. doi:https://doi.org/10.1016/j.pbiomolbio.2018.07.014
47. Streetz, K. L., Luedde, T., Manns, M. P., & Trautwein, C. (2000). Interleukin 6 and liver regeneration. *Gut, 47*(2), 309-312. doi:10.1136/gut.47.2.309
48. Susaki, Etsuo A., Tainaka, K., Perrin, D., Kishino, F., Tawara, T., Watanabe, Tomonobu M., . . . Ueda, Hiroki R. (2014). Whole-Brain Imaging with Single-Cell Resolution Using Chemical Cocktails and Computational Analysis. *Cell, 157*(3), 726-739. doi:10.1016/j.cell.2014.03.042
49. Thomas, C. A., Tejwani, L., Trujillo, C. A., Negraes, P. D., Herai, R. H., Mesci, P., . . . Muotri, A. R. (2017). Modeling of TREX1-Dependent Autoimmune Disease using Human Stem Cells Highlights L1 Accumulation as a Source of Neuroinflammation. *Cell Stem Cell, 21*(3), 319-331 e318. doi:10.1016/j.stem.2017.07.009

50. Tomlinson, B. L., Tomlinson, D. E., & Tassava, R. A. (1985). Pattern-deficient forelimb regeneration in adult bullfrogs. *Journal of Experimental Zoology, 236*(3), 313-326. doi:https://doi.org/10.1002/jez.1402360309
51. Tsai, S. L., Baselga-Garriga, C., & Melton, D. A. (2019). Blastemal progenitors modulate immune signaling during early limb regeneration. *Development, 146*(1), dev169128.
52. Wang, C., Nan, J., Holvey-Bates, E., Chen, X., Wightman, S., Latif, M. B., . . . Wang, Y. (2023). STAT2 hinders STING intracellular trafficking and reshapes its activation in response to DNA damage. *Proc Natl Acad Sci U S A, 120*(16), e2216953120. doi:10.1073/pnas.2216953120
53. Wang, X., Yang, C., Wang, X., Miao, J., Chen, W., Zhou, Y., . . . Liu, K. (2023). Driving axon regeneration by orchestrating neuronal and non-neuronal innate immune responses via the IFNgamma-cGAS-STING axis. *Neuron, 111*(2), 236-255 e237. doi:10.1016/j.neuron.2022.10.028
54. Wu, C. C., Kruse, F., Vasudevarao, M. D., Junker, J. P., Zebrowski, D. C., Fischer, K., ... & Bakkers, J. (2016). Spatially resolved genome-wide transcriptional profiling identifies BMP signaling as essential regulator of zebrafish cardiomyocyte regeneration. *Developmental cell*, *36*(1), 36-49.
55. Yang, H., Wang, H., Ren, J., Chen, Q., & Chen, Z. J. (2017). cGAS is essential for cellular senescence. *Proceedings of the National Academy of Sciences, 114*(23), E4612-E4620.
56. Yang, H., Wang, H., Ren, J., Chen, Q., & Chen, Z. J. (2017). cGAS is essential for cellular senescence. *Proc Natl Acad Sci U S A, 114*(23), E4612-E4620. doi:10.1073/pnas.1705499114
57. Ye, F., Zhang, G., E, W., Chen, H., Yu, C., Yang, L., ... & Guo, G. (2022). Construction of the axolotl cell landscape using combinatorial hybridization sequencing at single-cell resolution. *Nature Communications*, *13*(1), 4228.
58. Yu, Q., Walters, H. E., Pasquini, G., Singh, S. P., León-Periñán, D., Petzold, A., . . . Yun, M. H. (2022). Cellular senescence modulates progenitor cell expansion during axolotl limb regeneration. *bioRxiv*, 2022.2009.2001.506196. doi:10.1101/2022.09.01.506196

Figures

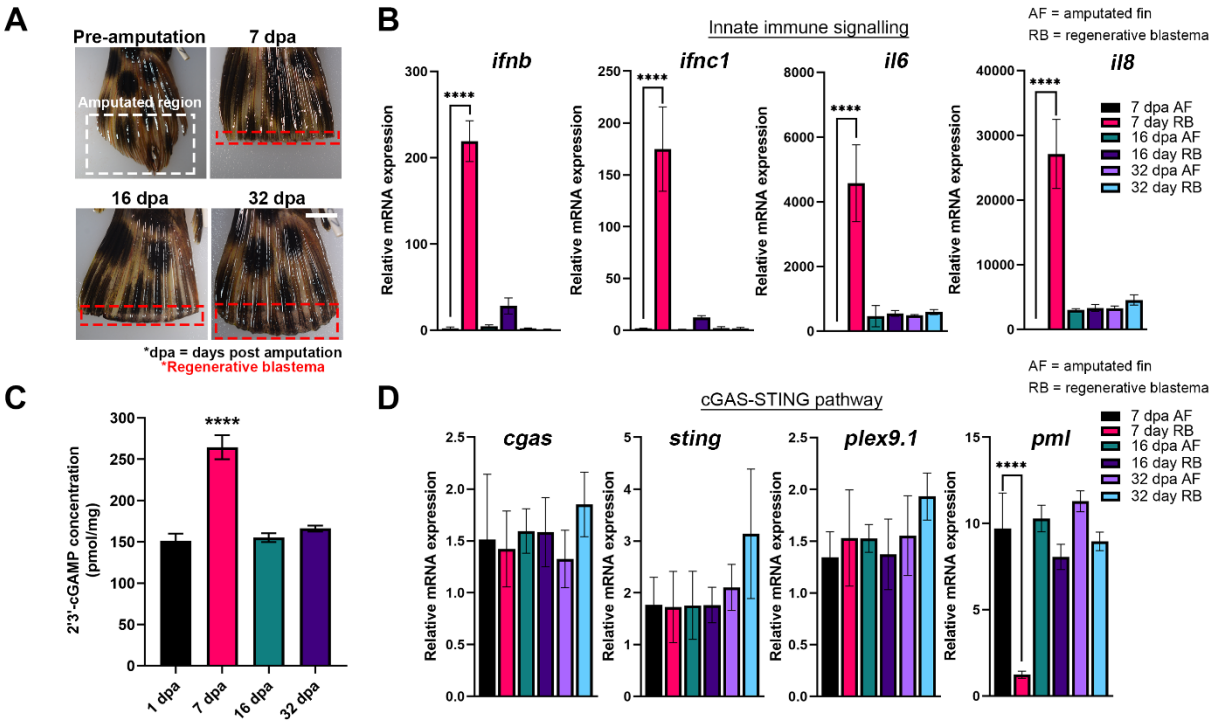

Figure 1. Early-stage gar regenerative blastema transition into a pro-inflammatory state with elevated cGAS activity. (a) Spotted gar caudal fins were amputated and regeneration was observed over a 32-day period, with regenerative blastema being collected at the indicated timepoints for molecular analysis. Scale bar indicates 1 cm **(b)** Interferons and Interleukins are upregulated in blastema at 7dpa before returning to baseline levels (n=3). Gene expression of *ifnb, ifnc1, il6* (Interleukin 6), and *il8* (Interleukin 8-like) was assessed and significantly different from the original amputated fin (AF) only a 7 dpa. **(c)** 2'3'- cGAMP levels are elevated specifically at 7dpa in regenerative blastema. 2'3'-cGAMP concentrations were determined from the same caudal fins used for RNA isolation. **(d)** Gene expression analysis of cGAS-STING pathway orthologs in gar indicate that *pml* is downregulated to facilitate immune signalling via the cGAS-STING axis. Variation between groups was assessed with a one-way ANOVA, with Tukey's post-hoc analysis for pairwise comparison between groups. ****$p < 0.0001$

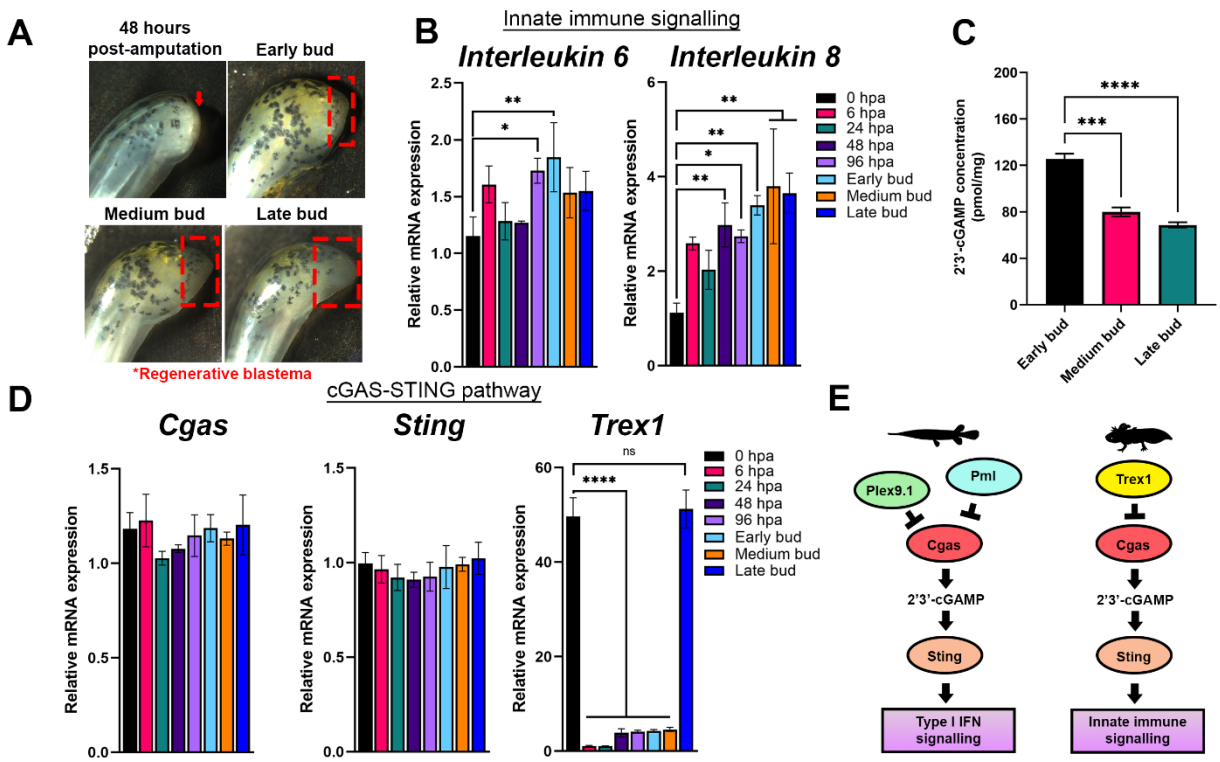

Figure 2. Trex1 is downregulated in the limb regenerative blastema of axolotl. (a) Axolotl limbs were amputated at the level of zeugopod and regeneration was observed at different stages of limb regeneration. **(b)** An increase in the expression of interleukin 6 (*Il6*) and interleukin 8 (*Il8*) was observed in the early stages of axolotl limb regeneration. Blastema from the regenerating limb was isolated within the first 96 hours and then at three different stages of limb regeneration (early, medium and late bud). **(c)** 2'3'- cGAMP levels are elevated in the early bud of the regenerating axolotl limb. 2'3'-cGAMP concentrations were determined from the same axolotl regenerative blastema used for RNA isolation. **(d)** Gene expression analysis of the cGAS-STING pathway orthologs in axolotl indicate that *Trex1* is downregulated during the stages of regeneration where cGAS activity is elevated. **(e)** Comparison of the cGAS-STING pathway in the spotted gar and axolotl. Variation between groups was assessed with a one-way ANOVA, with Tukey's post-hoc analysis for pairwise comparison between groups. *$p < 0.05$, **$p < 0.01$, ***$p < 0.001$, ****$p < 0.0001$

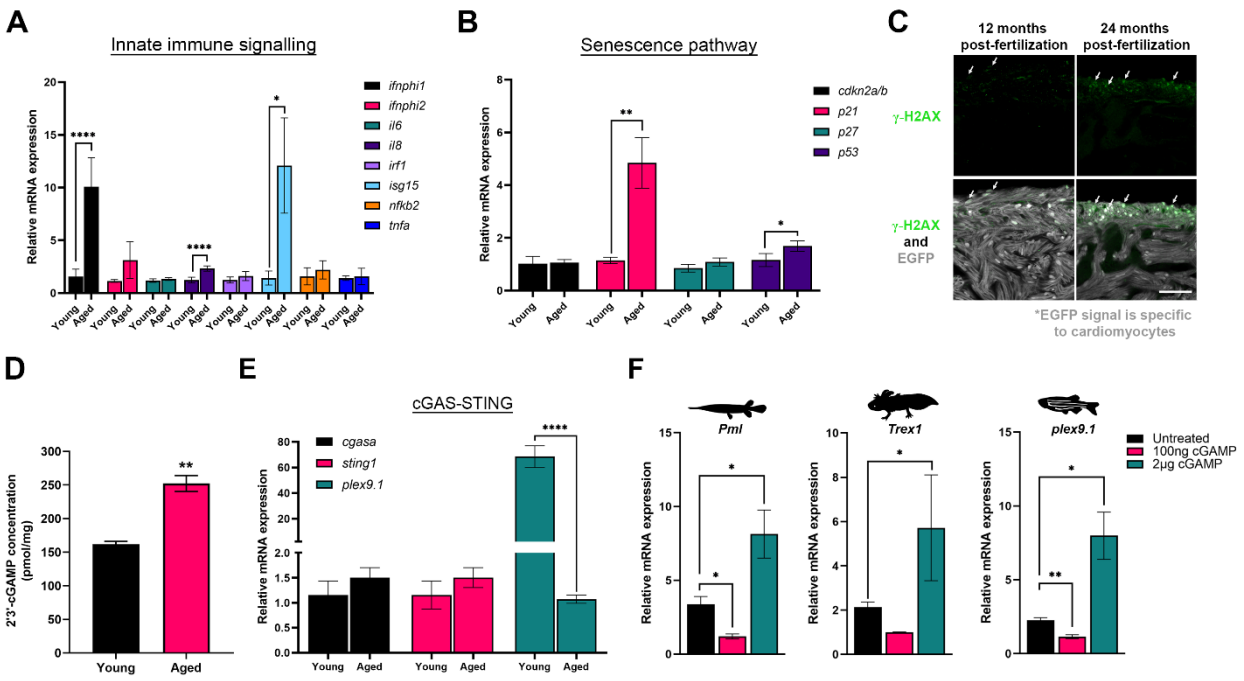

Figure 3. cGAMP is elevated in hearts from elderly zebrafish and regulates the expression of *pml, Trex1,* and *plex9.1*. (a,b) Gene expression analysis of zebrafish hearts from young and aged cohorts shows differences in innate immune signalling markers **(a)** and senescence markers **(b)**. **(c)** γ-H2AX foci, a marker of senescence are present in a greater abundance of cells in the hearts of elderly zebrafish. Myocytes were visualized using a *tg(myl7:eGFP)* reporter that the transgenic animals express. Scale bar is 50 µm. **(d)** cGAS activity is elevated in the elderly zebrafish. 2'3'-cGAMP concentrations were determined from individual hearts isolated from young and aged zebrafish. **(e)** Gene expression analysis of the cGAS-STING pathway orthologs in axolotl indicate that *plex9.1* expression is reduced in hearts from aged zebrafish. *cgasb* expression could not be detected in the zebrafish heart samples. **(f)** Treating cell lines derived from gar (GARL), axolotl (AL1) and zebrafish (ZKS) with cGAMP altered expression of the different cGAS suppressors. Gene expression in zebrafish hearts was compared with an unpaired, two-tailed Student's t-test (two-tailed). Variations between treatment groups was assessed with a one-way ANOVA, with Tukey's post-hoc analysis for pairwise comparisons between treatments. *p < 0.05, **p < 0.01, ****p < 0.0001

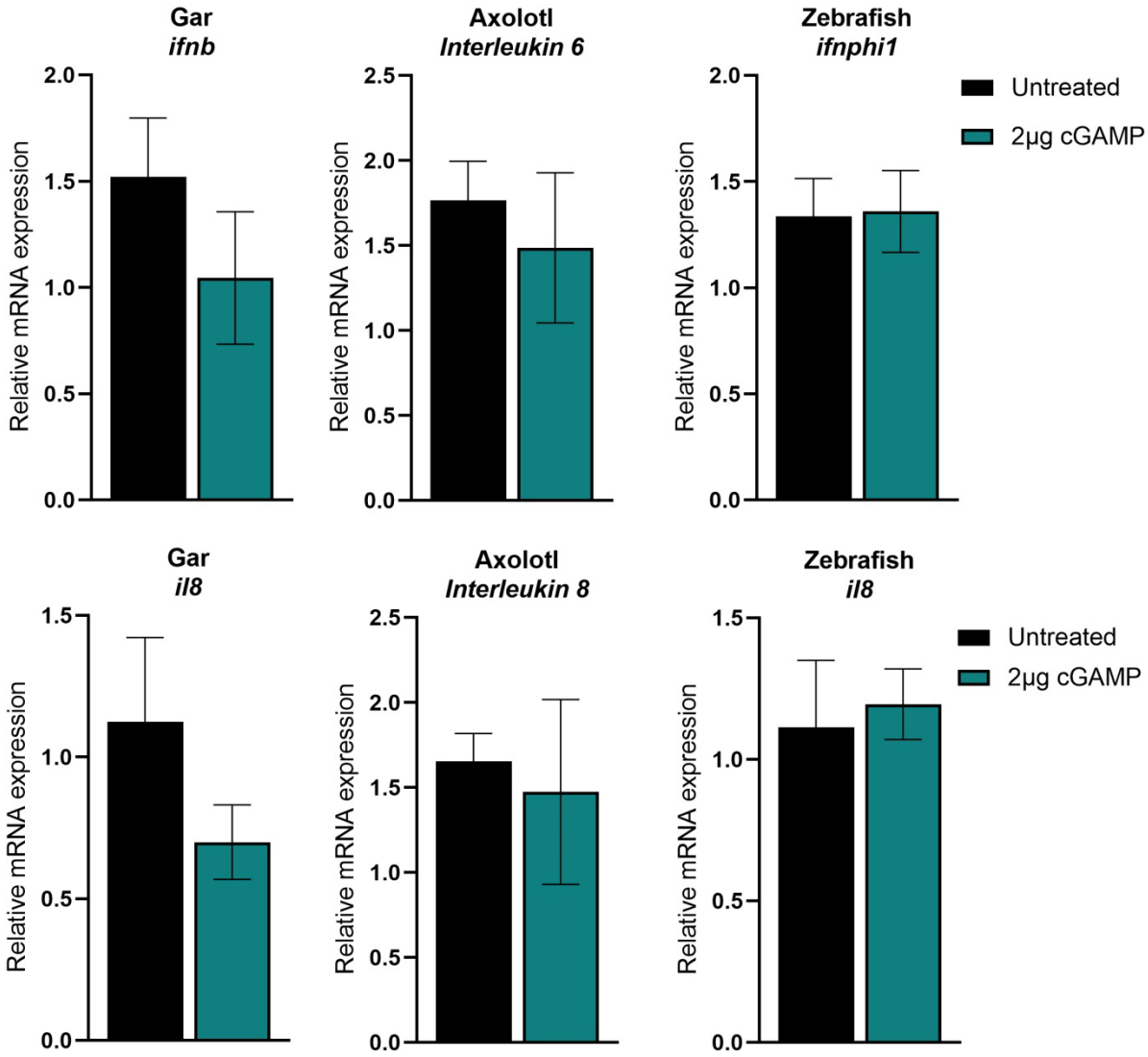

655

656 **Supplementary Figure 1. High levels of cGAMP transfection does not impact basal**
657 **interferon and senescence-related gene expression.** Gene expression analysis of different
658 interferon and senescence-associated genes in gar, axolotl, and zebrafish cell lines after
659 transfection with a high amount of 2'3'-cGAMP (2 µg). Gene expression was compared with an
660 unpaired, two-tailed Student's t-test (two-tailed).

661

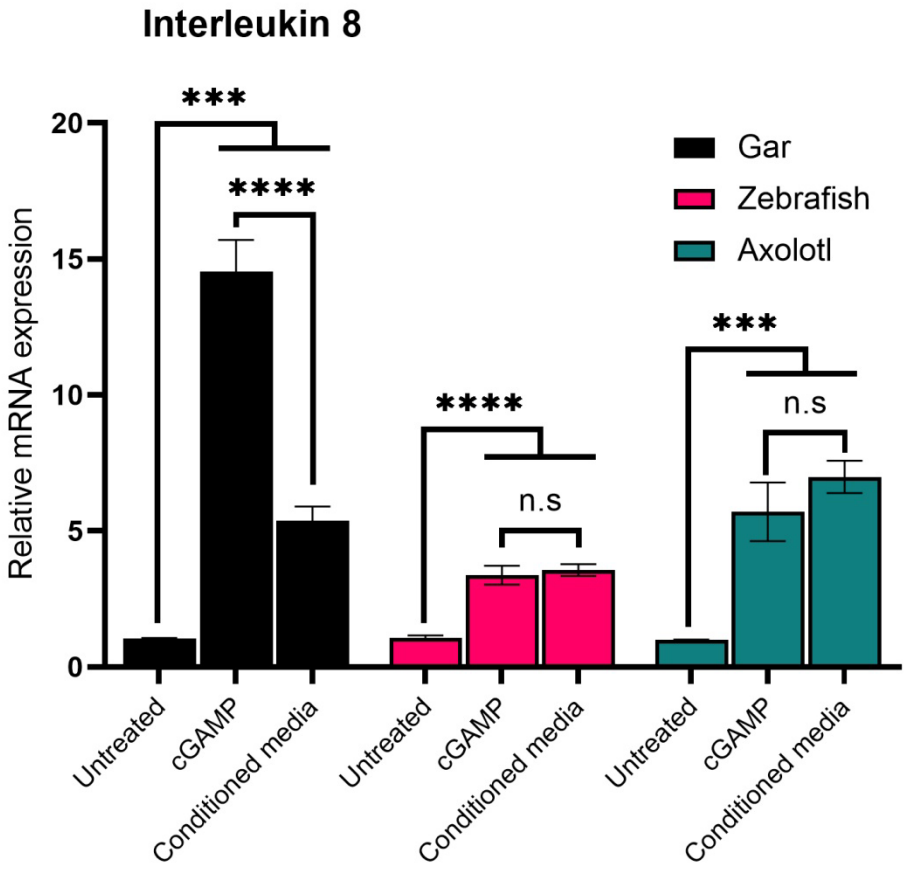

Supplementary Figure 2. Conditioned media from cGAMP treated cells induces the upregulation of interleukin 8. Gene expression analysis of interleukin 8 orthologs in gar, axolotl and zebrafish cell lines after transfection with 2'3'-cGAMP (100 ng) or with conditioned media from transfected cells. The conditioned media was obtained from each cell line 48 hours after 2'3'-cGAMP transfection and added to naïve cells with fresh media (1:1 ratio), then expression was analyzed 24 hours post-treatment. Variation between groups was assessed with a one-way ANOVA, with Tukey's post-hoc analysis for pairwise comparison between groups. ****$p < 0.0001$, ***$p < 0.001$

672

673

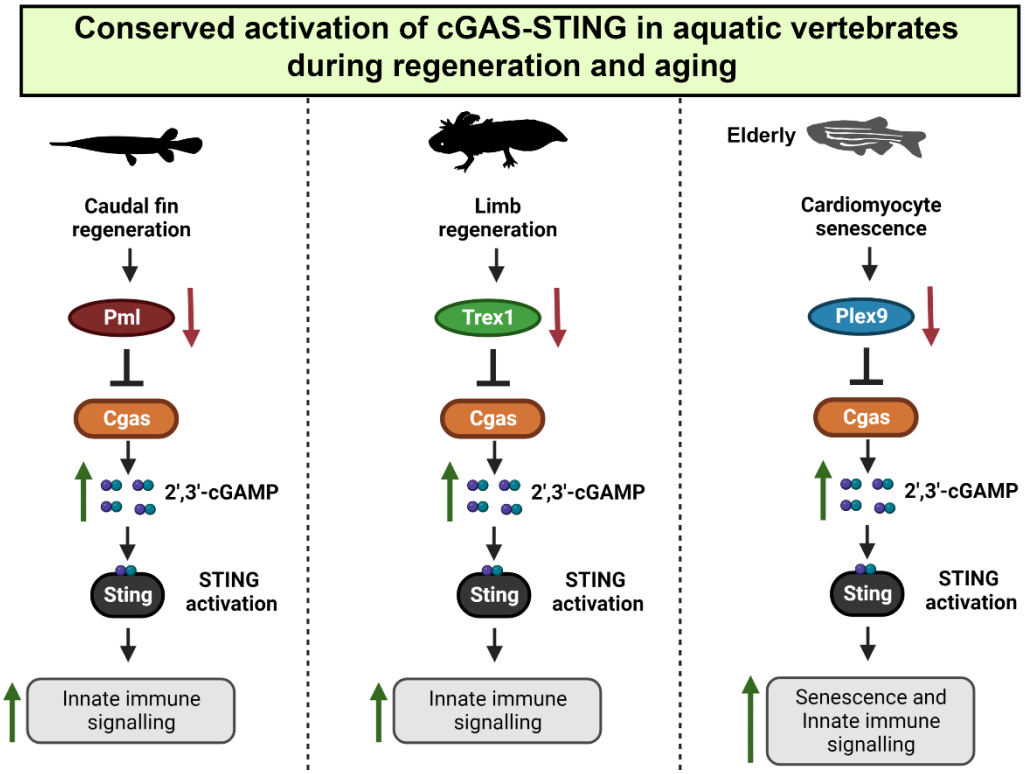

674

675 **Graphical abstract**

Suppressors of cGAS-STING are downregulated during fin-limb regeneration and aging in aquatic vertebrates

Sabateeshan Mathavarajah[1], Andrew W. Thompson[2,3,4], Matthew R. Stoyek[5], T. Alexander Quinn[5,6], Stéphane Roy[7], Ingo Braasch[3,4], Graham Dellaire*[1,8]

[1]Department of Pathology, Faculty of Medicine, Dalhousie University, Halifax, NS, Canada
[2]Department of Biological Sciences, Western Michigan University, Kalamazoo, MI, USA.
[3]Department of Integrative Biology, Michigan State University, East Lansing, MI, USA.
[4]Ecology, Evolution, and Behavior Program, Michigan State University, East Lansing, MI, USA.
[5]Department of Physiology and Biophysics, Dalhousie University, Halifax, Canada
[6]School of Biomedical Engineering, Dalhousie University, Halifax, Canada
[7]Department of Stomatology, Faculty of Dentistry, Université de Montréal, Montréal, QC, Canada.
[8]Department of Biochemistry and Molecular Biology, Dalhousie University, Halifax, NS, Canada

*Corresponding authors:

Dr. Graham Dellaire
Department of Pathology and Department of Biochemistry and Molecular Biology
Halifax, Nova Scotia, Canada
dellaire@dal.ca

Supplementary Material

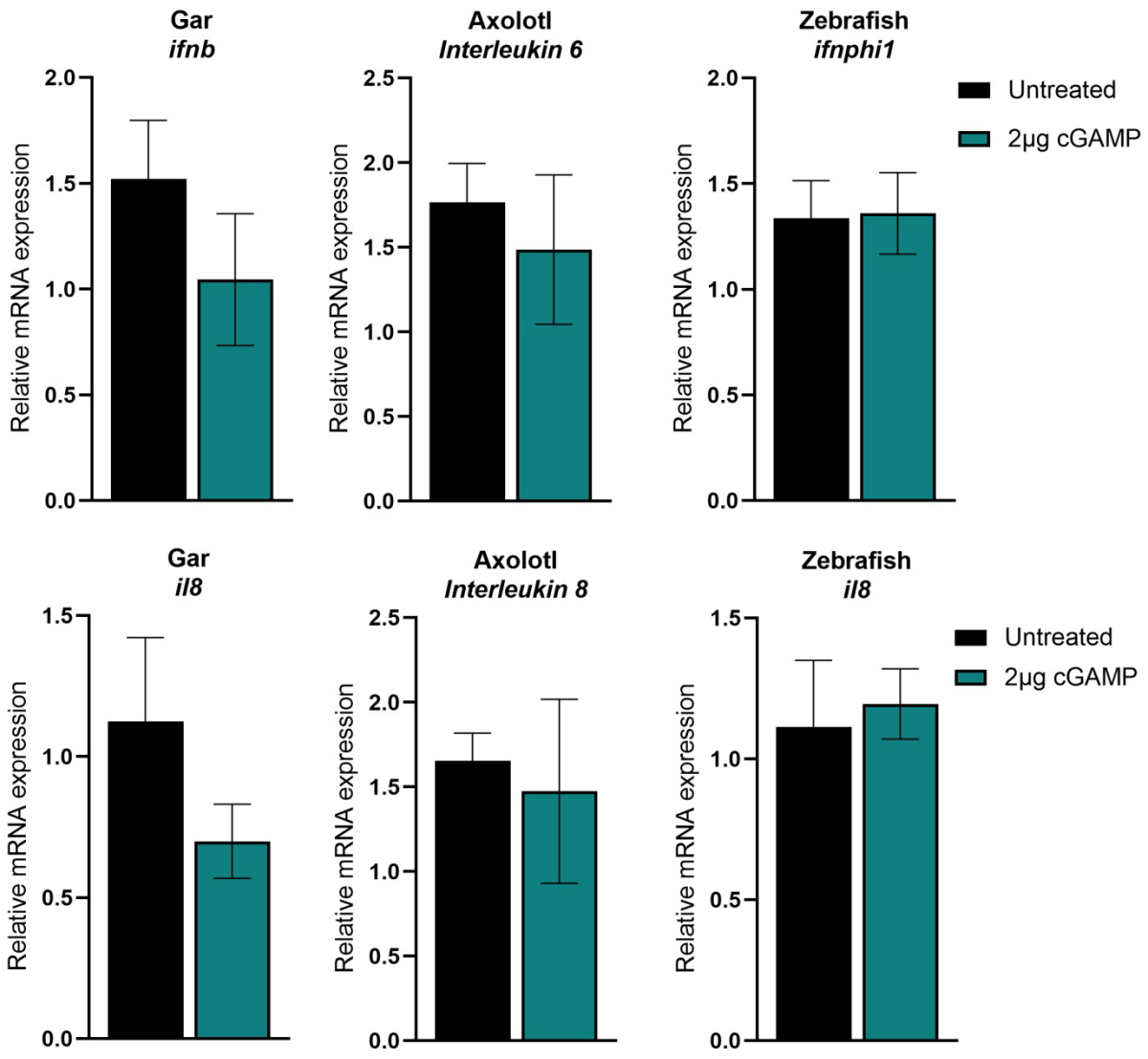

Supplementary Figure 1. High levels of cGAMP transfection does not impact basal interferon and senescence-related gene expression. Gene expression analysis of different interferon and senescence-associated genes in gar, axolotl, and zebrafish cell lines after transfection with a high amount of 2'3'-cGAMP (2 µg). Gene expression was compared with an unpaired, two-tailed Student's t-test (two-tailed).

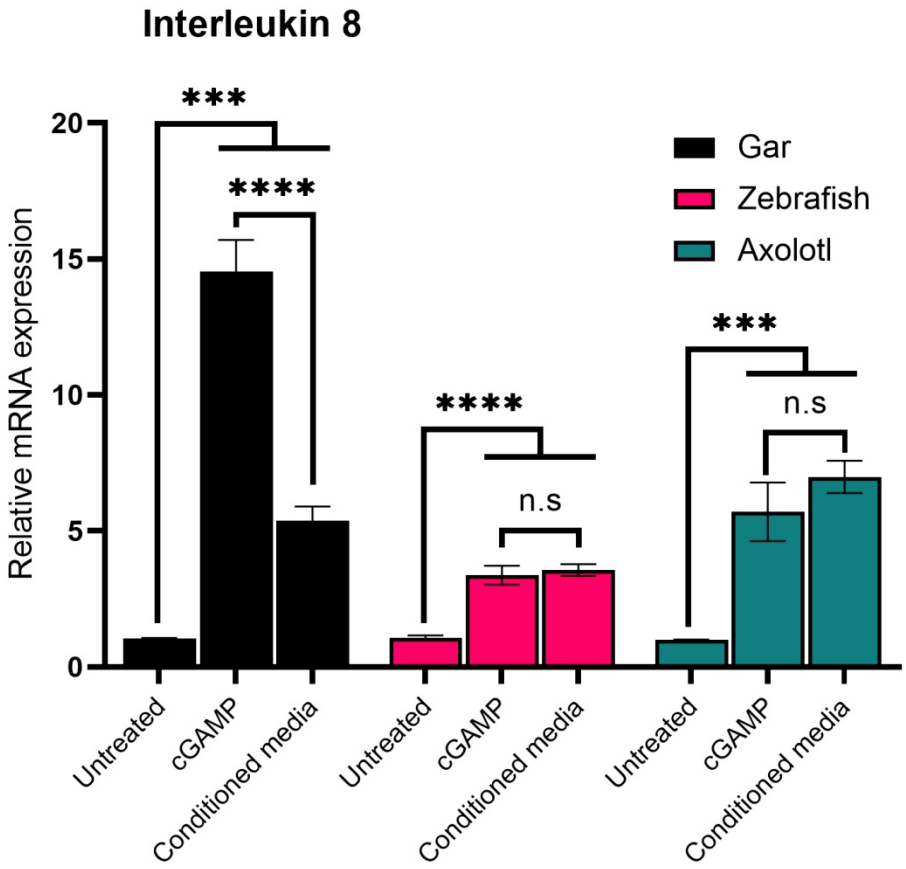

Supplementary Figure 2. Conditioned media from cGAMP treated cells induces the upregulation of interleukin 8. Gene expression analysis of interleukin 8 orthologs in gar, axolotl and zebrafish cell lines after transfection with 2'3'-cGAMP (100 ng) or with conditioned media from transfected cells. The conditioned media was obtained from each cell line 48 hours after 2'3'-cGAMP transfection and added to naïve cells with fresh media (1:1 ratio), then expression was analyzed 24 hours post-treatment. Variation between groups was assessed with a one-way ANOVA, with Tukey's post-hoc analysis for pairwise comparison between groups. ****$p < 0.0001$, ***$p < 0.001$

Supplementary Table 1

qPCR Primers

Species	Gene	Forward Sequence 5'-3'
Zebrafish	*cgasa*	GGCTACAGACCTCCCATACAA
	sting1	CGTGTCAAAGCTAATTCAAGATGT
	plex9.1	CAGTGGATCACGAGCGGTAA
	p53	GATGGTGAAGGACGAAGGAA
	p21	AACGCTGCTACGAGACGAAT
	p27	TGAAGCCTGGAACTTCGACT
	cdk2na/b	TGAACGTCGAGGATGAACTG
	irf1b	TGAAATCATGCCCGTGTCCA
	tnfa	ATGAAGCTTGAGAGTCGGGC
	isg15	AGAAGGGCCAGGTCAAAACT
	ifnphi1	AGAATGTGTGGCAAGATCCAC
	ifnphi2	ACTTGAGAGTATGGGCGGTC
	il6	TCAACTTCTCCAGCGTGATG
	il8	GAAAGCCGACGCATTGGAAA
	nfkb2	TGGCTGGAGCACTAAGGATG
	actb1	TTCACCACCACAGCCGAAAGA
	rplp0	CTGAACATCTCGCCCTTCTC
Spotted gar		
	plex9.1	ACAAAGACCGCGAATAAGAATTAA
	pml	TGGAGACCACAGGATTGGATCT
	cgas	GTTGGCCATCTTGCACCAAA
	sting	ATGGGGTTATGTGACCCTGC
	il6	CGCAGGTTACAGCTCTCCTC
	il8	CCGTTGAAGTCATTGCGCTT
	ifnb	AGACAGCTGAAAATGCCAAGAACG
	ifnc1	CTTACCGATGGCTCGCAGAATG
	actb1	GAAATTGCCGCACTGGTTGT
	gapdh	CTTTCAGGGTTCCCACTCCC
Axolotl		
	cgas	GATAGCGGCTGGTAGTTCCC
	sting	GTTCTCCCCTGTTCCCTTCC
	trex1	TAGCTGAAGGTATGGCCCCT
	gapdh	TTGTCCTACGTGTGCTGTCTGT
	rpl4	TGAAGAACTTGAGGGTCATGG
	il8	CCAGAGAGAGCAGGCAAATGG
	il6	ATGCCAGCCCAGTTCCAGACT

Reverse Sequence 5'-3'
CAGCTTGCACGGTGAACTTT
AGCAACGGCCAGAGTAAGAA
GAGACGCTCCCTCCGTTATG
AAATGACCCCTGTGACAAGC
CGCAAACAGACCAACATCAC
TGTGAATATCGGAGCCCTTC
AAGGTGCGTTACCCATCATC
TACCTGTGTGAATGGCCCAC
CCTGGGTCTTATGGAGCGTG
CGAGCTGTCTGCCTTTGAAA
CCTTGCGTTGCTTGCGATG
TCCGGATAACTGTCGTTGGC
TCTTTCCCTCTTTTCCTCCTG
TTAACCCATGGAGCAGAGGG
CCTCTCTGCTTTGGCTCCTC
TACCGCAAGATTCCATACCCA
TAGCCGATCTGCAGACACAC
CCACTTACAGCGGACAACTG
ACTGGCTCTGAGTGCAGAAG
ATTCGCCATGCATCTTTTGC
TACCCGGTGTAGAAGGACCA
GGCTGGCTAAGCACTTCTCT
AGTTGTTCCCCGTTTCACTTTT
TCATTTCGCTCCCTGCGCAA
TGTCCGATTCCTCAGAGC
ATACCAACCATCACACCCTGG
AGTCGGATGAGACGACCTGG
CGGGGTCCAGGAGTCTTTTC
GGTTATCCAATCGTCACGCC
ACCCTCTACCACGTACCTCC
TCACACAGTGCCAAGATAAGTGTT
CTTGGCGTCTGCAGATTTTTT
CACACAGAACCGACCGACCA
TGCCAGGGACTCGTATTTTGGT